13 Whole-Body PET Imaging Methods

Paul D Shreve

PET instrumentation has been available for over 25 years, yet the clinical applications of PET largely languished until the past decade. As the impediments to clinical PET [1] have fallen, the clinical value of the technology has become widely recognized and PET is now emerging as a mainstream diagnostic imaging modality. Over the past five years it has become clear PET using the glucose metabolism tracer [^{18}F]-fluorodeoxyglucose (FDG) will have a major role in the management of patients, particularly oncology patients. This has shaped the recent development of commercial PET tomographs and the evolution of clinical imaging protocols to accommodate rapid imaging of the whole-body (*c.f.*, torso) in a clinical setting.

Historical Development

Coincidence detection of positron radiotracers was accomplished as early as the mid 1960s using opposed detectors. Modern PET imaging systems are based on principles established by Phelps, Ter-Pogossian, and Hoffman at Washington University, St. Louis, in the early 1970s [2, 3]. The first commercial PET scanner, the ECAT II, introduced in the late 1970s, was capable of brain imaging and could accommodate the torso of a narrow patient [4]. Few of these were sold, as positron radiotracers were available only in research institutions with a cyclotron and appropriate radiochemistry facilities. The detection efficiency of these early tomographs was limited by the sodium iodide scintillator which has limited stopping power for the 511 keV annihilation photons. Scintillators with higher density and hence greater stopping power were investigated, including bismuth germanate oxyorthosilicate (BGO), gadolinium orthosilicate (GSO), and barium fluoride (BF), among others. In the late 1970s tomographs using the high density scintillators with attendant improvements in sensitivity and count rate capability were built in commercial and academic settings in limited quantities. These were dedicated brain PET tomographs, however, in part reflecting the exclusive research applications of PET at the time. A commercial PET brain tomograph using a high density scintillator (BGO), with at least a tentative intended clinical market niche, was introduced in 1978 [5].

Early success in the brain PET research encouraged some investigators and clinicians to contemplate analogous studies of tissue blood flow and metabolism in the heart and other organs of the body. Tomographs capable of accommodating the whole-body with more than just a few axial tomographic planes presented substantial cost barriers. The volume of scintillator and number of electronic channels required the development of block detectors, essentially very small Anger cameras, to limit the number of expensive photomultiplyer tubes and associated electronics [6]. In the early 1980s three commercial vendors introduced full ring BGO PET tomographs with gantry diameters capable of accommodating an adult torso. These scanners were capable of continuous data sampling of approximately 10 cm axial extent of the body in 15 or more contiguous transaxial planes. Transmission scanning using germanium-68 sources was incorporated in to the tomograph design to allow attenuation correction of the emission data. Each tomograph typically contained over 500 small photomultiplyer tubes, tungston axial septa, and substantial data processing hardware to reconstruct the thousands of coincidence lines. Due to the small commercial market at the time, such tomographs

were among the most expensive medical diagnostic imaging devices.

The commercial availability of whole-body PET tomographs in the 1980s allowed investigators with clinical interests to explore applications of PET to the heart, other major organs, and extra-cranial neoplasms. The theoretical potential of quantitative tracer kinetics, however, still remained strong, particularly among brain researchers. Hence, refinements in tomograph design in the mid 1980s retained the capacity for high count rate dynamic imaging of a limited axial field of view, accommodating the brain or heart, and transmission scanning for attenuation correction of the subject prior to injection of tracer. By the late 1980s, FDG imaging of extra-cranial neoplasms was emerging as a potentially more broadly applicable use of PET in clinical practice than imaging of the brain or heart. Initially, oncology imaging involved specific problem solving such as pulmonary nodules or masses identified on CT scans [7]. It soon became clear that a key advantage of FDG PET was detection of regional and distant metastatic disease not detected on conventional anatomical imaging [8]. While enthusiasm for the potential of quantitative kinetic analysis of imaging data applied to tumor imaging broadly, but most particularly to tumor response and drug evaluation remained [9], kinetic rate constants derived from quantitative dynamic imaging appeared to have no clear advantage over semi-quantitative or simple qualitative scan interpretation of FDG PET studies applied to simple diagnosis [10]. Consequently, for clinical diagnosis, FDG PET scan protocols emphasized static imaging of as much of the body as practical beginning roughly one hour after FDG administration.

With 10 cm axial field of view, as many as 7 bed positions would be required for a whole-body scan, and at 10 minutes emission acquisition per bed position, a whole-body scan required over one hour. Attenuation correction of the emission data required comparable time for the emission scans acquisitions, and since the transmission scanning had to be performed prior to tracer administration, an additional 50 minutes for FDG uptake and distribution prior to emission acquisitions was added for a total scanner time of 3 hours. As such, much of the body imaging in the 1980s was limited to non-attenuation corrected whole torso or attenuation corrected imaging limited to 2 or 3 bed positions, a procedure which generally could be accomplished in between 1 to 2 hours of scanner time. These protocols provided the early evidence of the importance of whole-body PET imaging for cancer staging [11]. The notion that clinical PET would involve primarily static imaging of a large axial extent (*i.e.*, the entire torso) and the need to reduce the expense of a clinical PET tomograph led to the development of innovative tomographs by the late 1980s employing conventional sodium iodide Anger cameras with 2.5 cm thick crystals in a hexagonal array [12]. To compensate for reduced sensitivity, such tomographs employed septa-less or 3D emission acquisition architecture with an extended axial field of view of 25 cm. Sealed point sources for singles transmission scanning were later developed, allowing the transmission scans to be performed even in the presence of tracer in the patient [13]. Whole-body attenuation scans could be performed in about an hour, although image contrast was degraded by the high fraction of scatter and random coincidence events consequent to the fully 3D emission acquisition. Partial ring rotating tomographs based on BGO detectors were also developed in an effort to reduce cost [14]. Again, 3D emission acquisition architecture to compensate for the reduced sensitivity was used along with sealed point sources for transmission scanning.

In the early 1990s, a new generation of full ring BGO commercial tomographs was introduced [15-17]. These tomographs used full ring BGO block detector design with a 15 cm axial field of view and removable axial septa such that they could be operated in both 2D and 3D acquisition modes [16–17]. Germanium-68 rod sources were used which allowed transmission scanning in the presence of tracer in the patient. Such "post injection transmission scans" made whole-body attenuation corrected imaging possible in roughly one hour on the BGO ring scanners (Fig. 13.1). Throughout the 1990s whole-body FDG PET imaging performed on the ring BGO and sodium iodide scanners provided the clinical experience and scientific evidence supporting government and private payment for clinical PET exams. Growing whole-body clinical applications increased the need to reduce imaging time while improving image quality. Much of the progress in improving image quality and reducing overall scan time involved improvements in image reconstruction algorithms (Fig. 13.2). Conventional filtered back projection algorithms were supplanted with statistical reconstruction algorithms using segmentation methods on the transmission scan data to reduce overall scan time on both emission and transmission acquisitions and yet still improve image quality on the whole-body scans [18, 19].

The need for attenuation correction on whole-body imaging remained somewhat controversial in the 1990s [20]. Transmission scan time added to overall imaging time, and noise from the transmission scan propagated into the final attenuation corrected emission scan, reducing lesion contrast. Further, many PET centers were performing whole-body non-attenuation corrected scans routinely with diagnostic results comparable to

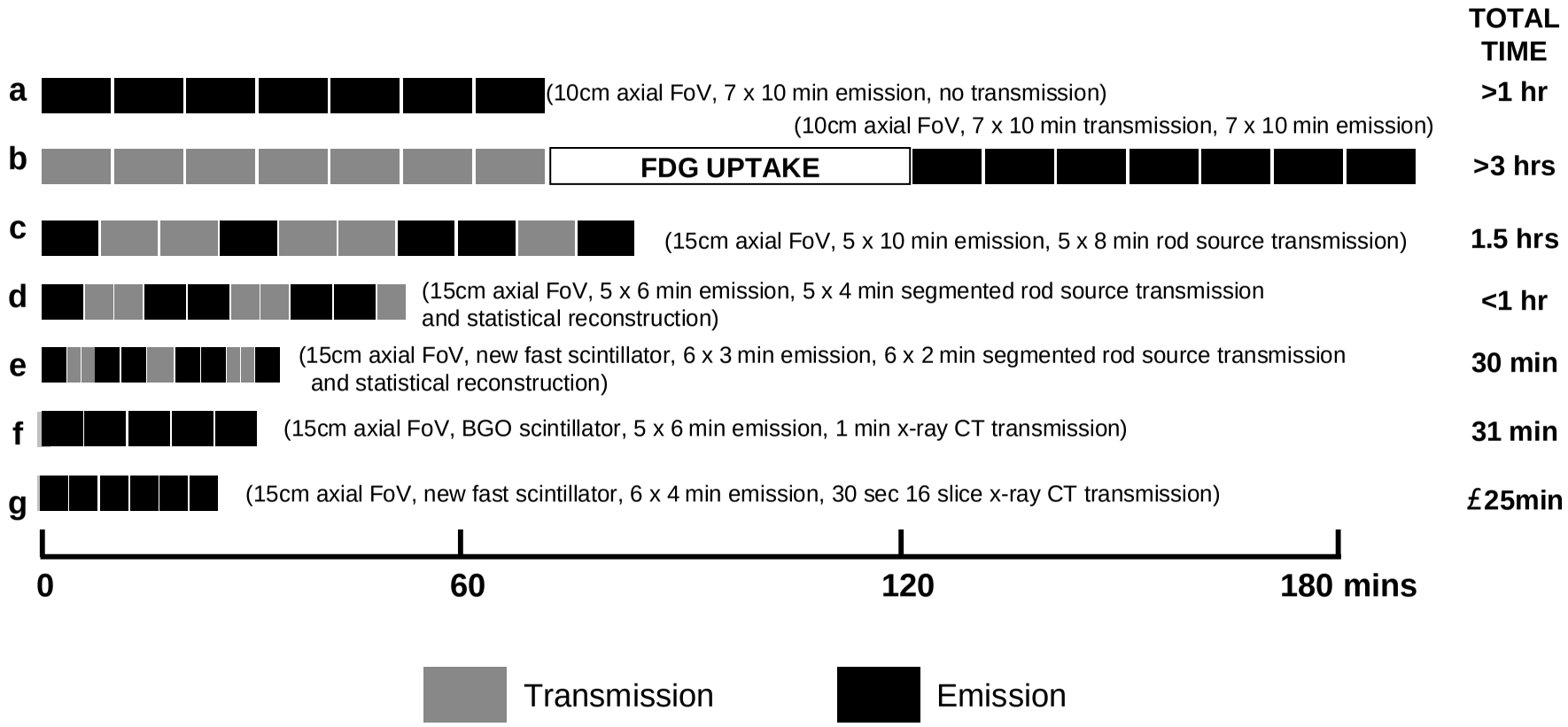

Figure 13.1. Whole body imaging protocols. Comparison of image acquisition protocols and scanner time required to complete a whole body acquisition. Ring tomographs in the 1980s were limited by a 10 centimetre axial field of view and transmission scanning they could only be used prior to tracer administration. A whole-body scan of roughly 70 cm axial length thus required more than one hour without attenuation correction (**a**), and an impractical three hours with attenuation correction (**b**). By the early 1990s, tomographs with longer axial fields of view (15 cm BGO and 25 centimetre NaI(Tl)) and the capability to perform transmission acquisition after tracer injection became available. These could complete a 70 cm examination with attenuation correction in about 1.5 hours (**c**). Refinements in image reconstruction permitted reduction in emission and transmission acquisition times, allowing for whole body image acquisition time to be reduced to less than one hour by the late 1990s (**d**). New detector technology permitting 3D image acquisition following injection of 400–550 mBq of tracer now allows whole body emission and transmission image acquisition of 70 centimetre axial length in about 30 minutes (**e**). Likewise combined PET/CT tomographs reduce whole body imaging time by markedly reducing transmission scan time, allowing whole body attenuation corrected studies in 30 minutes or less (**f** and **g**). Note that the actual imaging time is slightly greater than acquisition time alone due to additional time needed for scanner bed and transmission source movement. There is greater field of view overlapping in 3D acquisition mode than 2D mode, hence the extra bed position in (**e**).

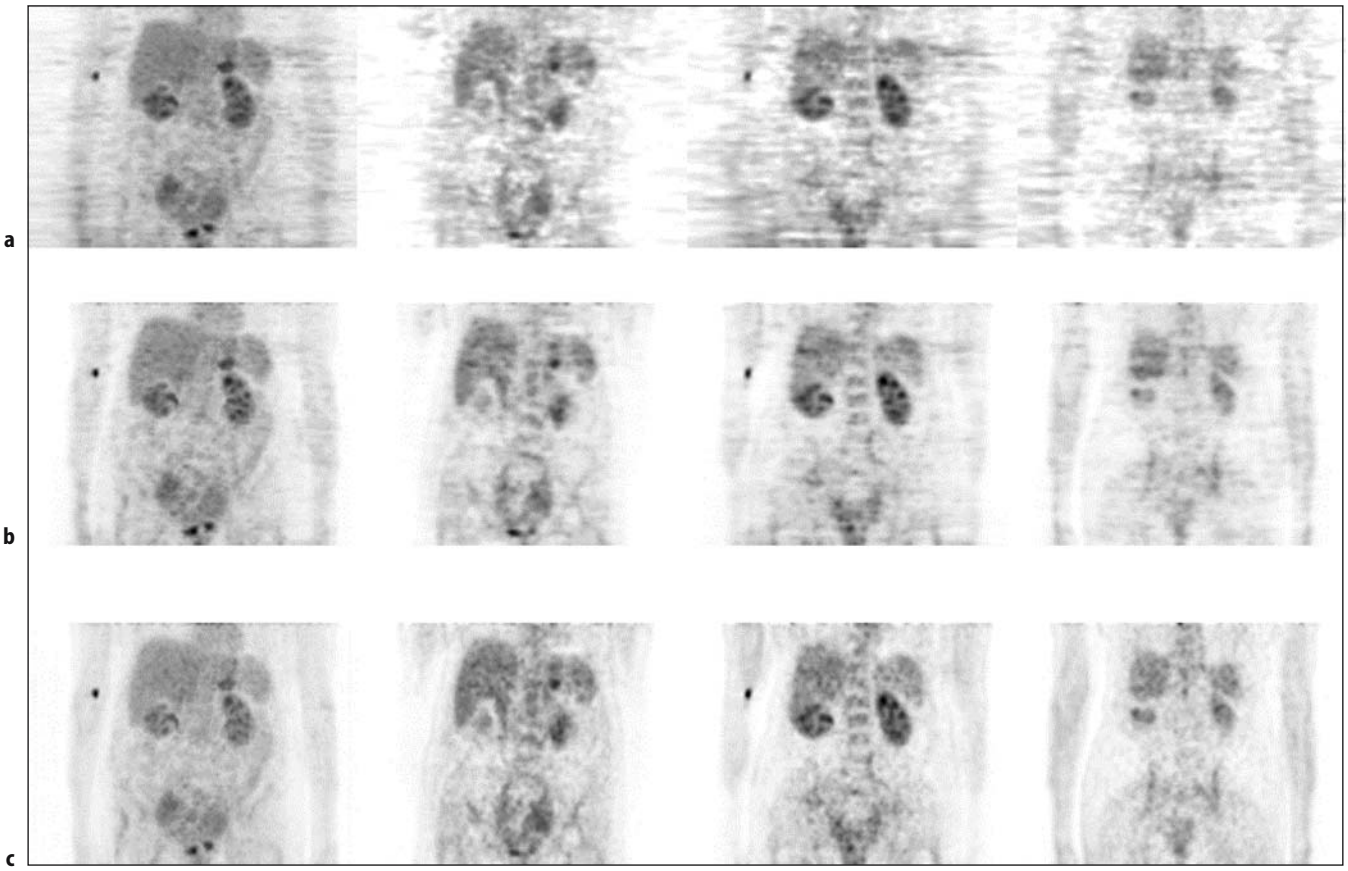

Figure 13.2. Comparison of image reconstruction methods. Substantial improvements in whole-body FDG PET image quality have occurred due to refinements in image reconstruction algorithms. Shown above are anterior projection images and coronal image sections of the abdomen and pelvis, with acquisition beginning about one hour after FDG administration. Two-dimensional acquisition was used (six minutes per bed position) and transmission scanning was performed with rotating Ge-68 rod sources (four minutes per bed position). The same emission and transmission data are shown after reconstruction by filtered back-projection (**a**), by statistical or iterative reconstruction using ordered subset expectation maximization (OSEM) (**b**), and by attenuation-weighted statistical reconstruction (**c**). [Courtesy of Technical University of Munich and CPS Innovations Inc., Knoxville, Tennessee.]

centers using attenuation corrected protocols. Never the less, the need for anatomical correlation and the diminishing time and noise penalty for attenuation correction have resulted in most centers now performing attenuation correction routinely on whole-body protocols. Further, refinements in attenuation weighted statistical reconstruction algorithms which allow for further improvements in image quality (Fig. 13.2) require the anatomical map of a transmission scan.

Early commercial PET tomograph design relied on axial septa to reduce random and scatter coincidences and constrain image reconstruction to a series of 2D tasks which could be solved in a reasonable time using existing computational hardware and software. By the late 1980s and throughout the 1990s efforts to move towards 3D imaging in the body accelerated as image reconstruction computational hardware and software advanced [21, 22]. By expanding the number of accepted out of plane coincidence events, tomograph sensitivity increases dramatically. Removing the axial septa altogether also reduces cost and permits a wider gantry aperture, improving patient comfort. Unfortunately random and scatter coincidence events increase even more so than the true coincident events, and degrade image contrast unless successfully corrected. The full potential in increased sensitivity is also not fully realized as detectors with slow light decay scintillators such as BGO and sodium iodide cannot accommodate the high photon flux associated with patients given FDG in excess of approximately 350 MBq. Due to the relative limited scatter medium and out of field source of random coincidences, 3D acquisitions of the brain are readily accomplished and have allowed for reduced imaging time and improved image quality. 3D acquisitions in the body however have yielded poorer image contrast than 2D acquisitions, particu-

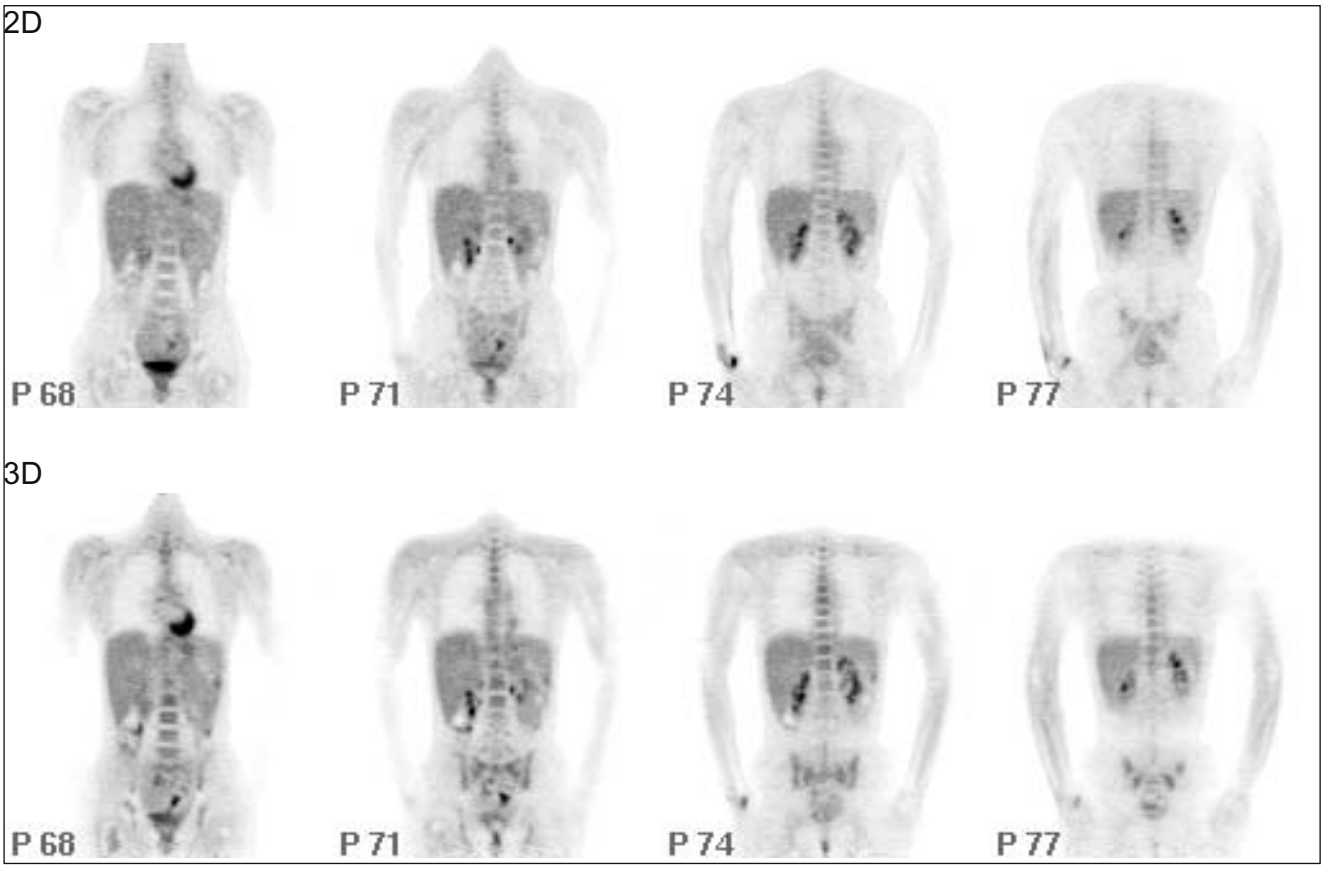

Figure 13.3. Whole-body 2D vs 3D image acquisition. Emission acquisitions can be performed in a 2D mode in which axial septa are employed to permit only a narrow angle of photon acceptance, or a 3D mode in which axial septa are absent. The 3D mode allows higher overall sensitivity but requires image reconstruction algorithms that are capable of correcting for the much higher contributions of random coincidences and scattered photons. Image reconstruction algorithms now allow reconstruction of images acquired in 3D mode which are comparable to 2D images in quality, but require a lower injected dose or shorter acquisition time due to the higher sensitivity. Shown above is a comparison of FDG PET whole-body coronal images of the same patient obtained on a BGO tomograph, first in 2D mode and then in 3D mode . Total image acquisition times were comparable, since the 3D image was obtained after a longer tracer decay time. [Courtesy of Kettering Memorial Hospital, Kettering, Ohio, and CPS Innovations Inc., Knoxville, Tennessee.]

larly evident in larger patients. Refinements in randoms and scatter correction have shown improvements in whole-body 3D acquisitions such that they are now becoming comparable to high quality 2D studies performed on full ring BGO tomographs (Fig. 13.3).

Current Trends in Whole-Body Tomographs

Body oncology applications of clinical PET are driving scanner technology to further improve image quality for small lesion detection and reduce scanning time for faster patient throughput in the clinic. Such improvements will require higher sensitivity for shorter emission acquisition times and shorter transmission scan time. High sensitivity can be achieved in 3D mode if a tomograph can accommodate the markedly increased detector event rates for higher true coincident count rates while the scatter and random coincident contributions to the final reconstructed images are minimized. Scintillators with faster light decay times such as lutetium oxyorthosilicate (LSO) or gadolinium oxyorthosilicate (GSO) and improved detector system energy resolution will allow for further increments in performance. Faster light decay times permit much higher detector count rate capability permitting full 3D body emission image acquisitions at patient tracer doses limited by tracer dosimetry rather than detector count rate capability (Fig. 13.4). For example, a full ring LSO tomograph based on conventional BGO design, has equivalent sensitivity to the BGO tomograph, but much higher count rate capability, allowing 3D body

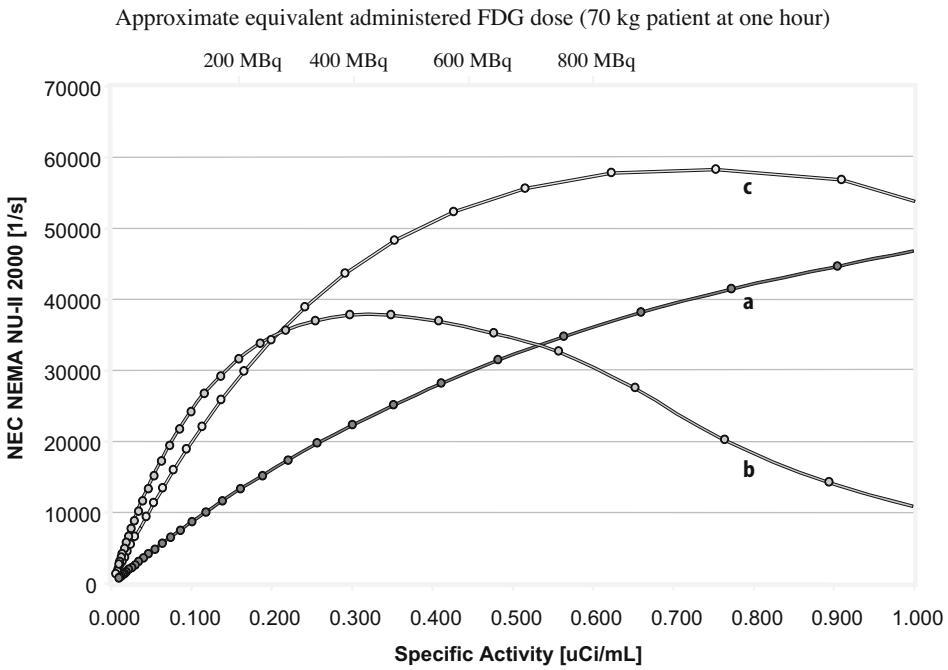

Figure 13.4. Count rate performance of BGO vs LSO detector materials. A useful method of evaluating and comparing PET tomograph performance is the noise equivalent count rate curve. A standard cylindrical phantom containing tracer in water is imaged, and the true, random and scattered coincidence counts as measured by the tomograph are recorded. Using a standard formula, the noise equivalent count rate (NEC) is computed. The test is performed over a range of tracer activity in the phantom, and a curve is generated showing the increasing NEC with increasing tracer activity. The NEC is generally limited by the tomograph count-rate capability and the exponential increase in random coincidence rate with increasing dose. For these reasons, the NEC curve reaches a maximum and then declines. The NEC is an approximate measure of useful coincidence events. Shown above are NEC curves for (**a**) 30 mm-deep BGO detectors in 2D mode and (**b**) 3D mode, compared to (**c**) 25 mm-deep LSO detectors in 3D mode. The BGO detectors in 2D mode do not reach a maximum at these levels of activity, while the same detectors in 3D mode quickly reach a maximum NEC and then decline due to increasing random coincidences and count rate limitations. With BGO, the 3D mode does not allow higher count rates and shorter imaging times but does permit use of lower tracer doses. Because of faster light decay and a narrower coincidence time window, the LSO detectors in 3D mode permit higher count rates with half the relative random coincidence contribution of the "slower" BGO. Consequently, a higher maximum NEC is achieved with the LSO detectors in 3D mode, even though the BGO detectors in 3D mode have slightly higher sensitivity. The approximate range of tracer concentration in the body of a 70 kg adult, one hour after administration of 200 to 800 MBq FDG is noted for comparison. [Courtesy of CPS Innovations, Knoxville, Tennessee.] (Reproduced from Valk PE, Bailey DL, Townsend DW, Maisey MN. Positron Emission Tomography: Basic Science and Clinical Practice. Springer-Verlag London LTD, 2003, p. 486.)

image acquisitions with patient does of FDG up to 700 MBq. Random coincidence contributions can be reduced by the very narrow coincidence timing window (4–6 nanoseconds) and scatter coincidences are at least partially corrected using anatomy based algorithms. Contribution of scatter coincidences to image degradation can be reduced by improvements in effective energy resolution both due to properties of scintillation crystals and sampling and analysis of scintillator light output [23], in addition to attenuation weighted scatter correction algorithms [24]. The high count rate capability of fast light decay scintillators accommodates higher activity transmission scan sources allowing for emission image acquisitions as short as 1 minute per bed position. Thus with emission scan acquisitions shortened to 3 , or even 2 minutes per bed position and high count rate transmission scans shortened to 1 minute per bed position, high image quality whole-body exams can be performed in under 20 minutes using a 15 cm axial field of view tomograph (Fig. 13.5). The shortened acquisition times in turn further improve image quality by minimizing patient movement during scan acquisition.

The need for anatomical correlation in both interpretation and therapy planning is also driving the merging of PET and CT tomograph technology (25, 26). The X-ray CT attenuation map, which can be scaled to a 511 keV transmission map [26] provides a very rapid transmission scan with minimal noise. Effectively the transmission scan contribution to overall scanning time is reduced to less than one minute for a whole-body exam. A conventional full ring BGO detector of 15 cm axial field of view in the PET/CT configuration can acquire a whole-body diagnostic CT and attenuation corrected PET in about 30 minutes (Fig. 13.6). With fast crystal detector PET tomographs operated in full 3D mode in a PET/CT configuration, whole torso have been reported in under

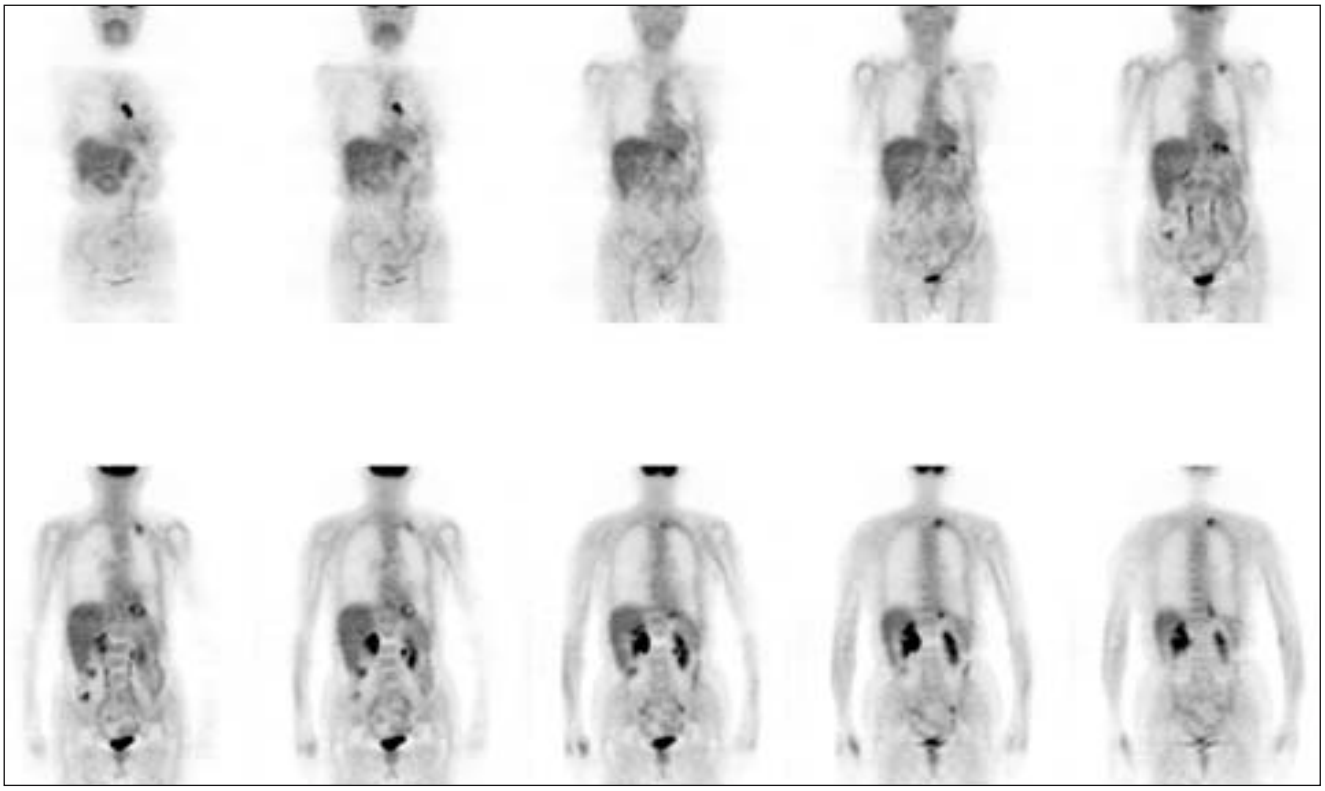

Figure 13.5. Whole-body images obtained with a full-ring LSO tomograph of 15 cm axial field-of-view, operating in 3D mode. Attenuation-corrected whole-body images were obtained in less than 25 minutes, using a dose of 500 MBq FDG. [Courtesy of Northern California PET Imaging Center, Sacramento, California.] (Reproduced from Valk PE, Bailey DL, Townsend DW, Maisey MN. Positron Emission Tomography: Basic Science and Clinical Practice. Springer-Verlag London LTD, 2003, p. 487.)

10 minutes total scan acquisition time [27]. The advantages of accurately registered and aligned PET metabolic and CT anatomical images for both diagnosis and radiation therapy planning are already becoming clear [28–31]. As predicted [26], the grafting of the PET metabolic images on the familiar CT anatomical images is speeding acceptance of PET as a mainstream imaging modality among radiologists, oncologists and surgeons. Already the majority of PET scanners sold are in the configuration of a PET/CT scanner, and it appears the standard modality for body oncology imaging will be the combined PET/CT. Perhaps the most important consequence of this evolution of body PET imaging to PET/CT is the merger of metabolic and anatomical diagnosis into one imaging procedure and one overall medical imaging interpretation.

Whole-Body Imaging in Oncology

Overview

Presently whole-body FDG imaging protocols for oncology applications takes full advantage of the recent developments in tomographs and image reconstruction. For most extra-cranial malignancies, the goal is to image the entire torso, from skull base to pelvis within one hour or less of scanner time, and in fact with recent developments in PET tomograph detector technology and combined PET/CT tomographs, imaging of the entire torso in under 30 minutes is becoming routine. The brain is usually not included in the axial field-of-view for imaging extra-cranial malignancies as

a FDG PET **b** CT **c** Fused : 58% PET/ 42% CT

Figure 13.6. Whole-body images obtained with a combined PET/CT tomograph. Whole-body images obtained with a full-ring BGO tomograph with 15 cm axial field of view, operating in 3D mode and using CT image data for attenuation correction. (**a**) Attenuation-corrected coronal whole-body PET image, and (**b**) coronal reconstruction of diagnostic CT data, obtained sequentially in 30 minutes total, producing highly registered metabolic and anatomic images. (**c**) fused PET and CT images. [Courtesy of Memorial Sloan-Kettering Cancer Center.]

FDG uptake in the brain is of a level found in most malignant neoplasms, hence detection of brain metastases is still best accomplished by contrast enhanced CT or MR. One notable exception is melanoma, a neoplasm with such intense FDG uptake and propensity for widespread and unpredictable metastatic sites, that brain metastases can be detected on FDG PET, and therefore many centers include the entire head in whole-body imaging of melanoma patients. For lung cancer and oesophageal patients, the top of the axial field-of-view should include the base of the neck, for head and neck cancer and lymphoma patients up to the skull base. Patients with cancers originating in the gastrointestinal and genito-urinary tract require body positioning to insure the entire pelvis, to below the level of the pubic symphysis, in addition to the abdomen and chest is included. In lymphoma patients the caudal extent of axial field-of-view typically includes the upper thighs to insure inguinal lymph nodes are included. Again, with melanoma patients, some or all of the lower extremities will be included at some centers, often using shorter imaging acquisition times for the lower extremities. Hence for most patients 70–80 cm axial extent imaged will comprise a whole-body study, for lymphoma and melanoma patients 90–120 cm.

Patient Preparation

Patient preparation for whole-body FDG PET examinations is an essential part of the procedure both to optimize image quality and to minimize physiological variants and artefacts [26]. Patients should be fasted a minimum of 4 hours to insure serum glucose and endogenous serum insulin levels are low at the time of FDG administration. Typically patients are fasted overnight with no breakfast for morning appointments, and can have a light breakfast, but no subsequent lunch or snakes for afternoon appointments. Glucose competes with FDG for cellular uptake, and there is some evidence elevated serum glucose will lower observed FDG uptake in malignant neoplasms [33]. Equally significant, elevated serum insulin promotes FDG uptake in the liver and muscle. Hence a recent carbohydrate containing meal (even a snack) or administration of exogenous insulin in attempt to lower blood glucose levels prior to FDG administration can yield extensive muscle uptake (Fig. 13.7). Such muscle uptake will not preclude evaluation of centrally located abnormalities such as lung nodules or mediastinal lymph nodes, but can potentially reduce conspicuity of osseous and peripheral lymph node basin involvement and reduce available circulating FDG for tumor uptake. Myocardial FDG uptake will be absent given a sufficiently long fast (18–24 hours) due to the shift to fatty acids as an energy source. With shorter fasts (which patients can tolerate such as overnight) myocardial FDG uptake will vary from uniform intense, to irregular, to absent in largely unpredictable patterns among patients. Hence the goal of fasting is not ordinarily to eliminate the myocardial FDG uptake.

In general, a serum glucose level under 150 mg/dL at the time of FDG administration is preferred, with less than 200 mg/dL acceptable. With serum glucose levels above 200 mg/dL, noticeable degradation in image quality due to reduced tissue uptake of FDG and sus-

tained blood pool tracer activity can occur. It is relatively easy to measure serum glucose prior to FDG administration, and this is routine in many centers. Use of exogenous insulin to reduce serum glucose immediately prior to FDG administration is not generally indicated, as this will result in accelerated FDG uptake in muscle and the liver. It is much preferred to manage known diabetic patients such that at the time of FDG administration, serum glucose levels are under roughly 150 mg/dL. This must be arranged in consultation with the patient and the physician treating their diabetes, as the strategy used will depend on the patient's treatment regimen and history of serum glucose control. For example, patients who are non-insulin requiring may present with an acceptable serum glucose levels with an overnight fast, while insulin requiring patients may need a fraction of their usual morning dose of short acting insulin in addition to the overnight fast. For patients with poor serum glucose control, the goal is not entirely normal serum glucose, simply less than roughly 150 mg/dl, as there is a risk of hypoglycemia. If a patient is found to be hypoglycemic at the time of FDG administration, and is not symptomatic, it should be noted that approximately 30 minutes after FDG administration, much of the FDG uptake has occurred, and serum glucose can be subsequently by normalized without compromising the examination. Simple ingestion of a sweet juice drink is often sufficient to insure adequate glucose levels for the duration of the examination. Patients without a diagnosis of diabetes mellitus will occasionally present for an FDG PET scan with abnormal elevated fasting serum glucose, but this rarely exceeds 150 mg/dL, much less 200 mg/dL. When patients do present with and abnormally diffuse increased muscle and liver uptake, it may well reflect a recent snack (Fig. 13.7); hence it is important to emphasize the meaning of fasting for the exam at the time the patient is scheduled.

Hydration prior to FDG administration will, as with any tracer cleared by urinary excretion, facilitate tracer clearance from blood pool and the urinary tract. Patients should be encouraged to drink plenty of water, but only water (no sugar containing beverage), prior to FDG administration. After FDG administration

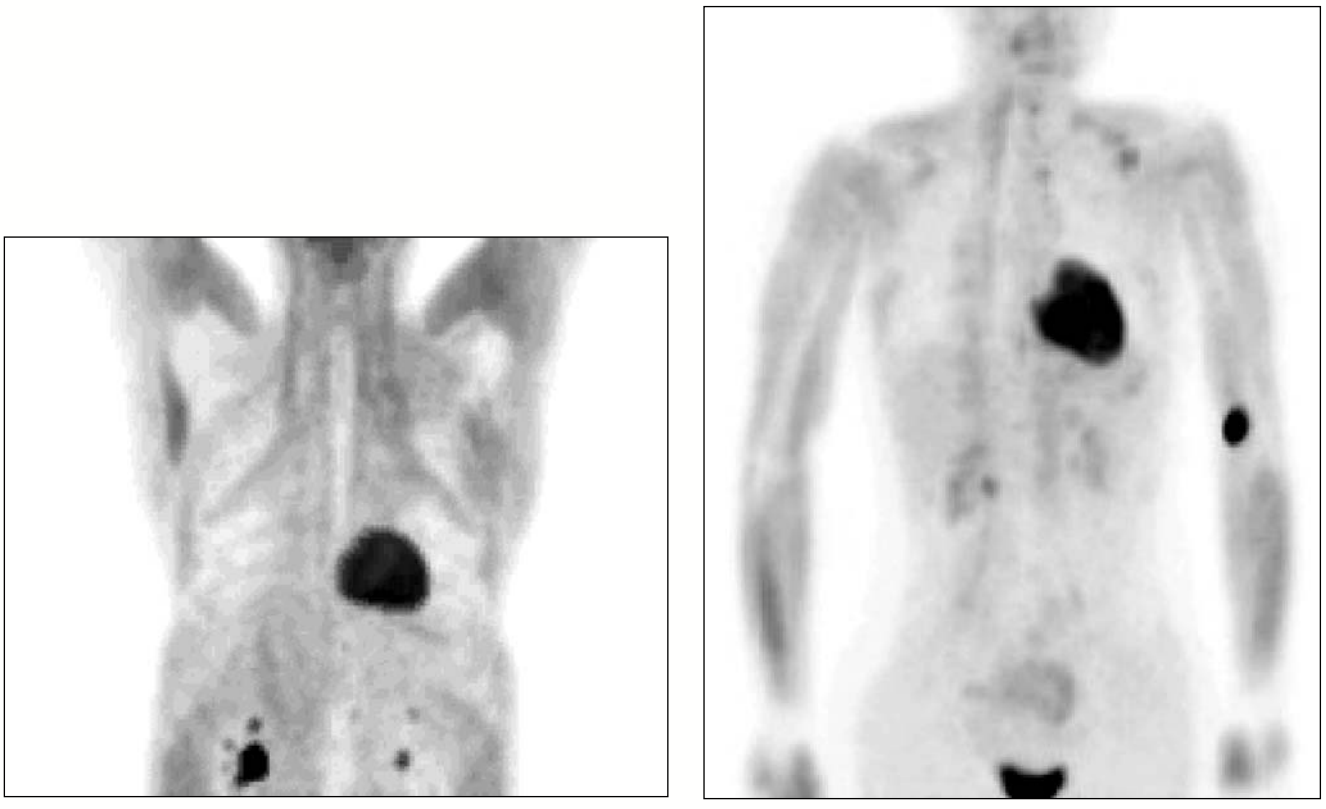

a b

Figure 13.7. Effect of exogenous and endogenous insulin. Whole-body anterior projection images of (**a**) a patient given 10 units of regular insulin intravenously prior to FDG administration, attempting to normalize a serum glucose level of 180 mg/dL, and (**b**) a patient who fasted overnight but ate an apple and half a granola bar prior to FDG administration. In both cases there is extensive skeletal muscle uptake, uniform and symmetrical, due to the action of insulin.

drinking, chewing or even talking must be eschewed for at least approximately 30 minutes to avoid muscle FDG uptake. The presence of urinary tracer in the upper urinary tract and bladder can be confounding [33]. Pooling of urinary tracer in the renal calyces can mimic a renal or adrenal mass, while urinary tracer in an extra-renal pelvis or isolated down the course of the ureters can mimic FDG avid retro-peritoneal lymph nodes. Such mimics involving urinary tracer activity are less problematic with properly registered and aligned PET and CT images such as generated on combined PET/CT scanners. Intense urinary tracer activity in the bladder can result in reconstruction artefacts limiting evaluation of adjacent structures, including uterus, adnexa, prostate, rectum and obturator nodal groups.

It is possible to minimize or largely eliminate urinary tracer activity by hydration and use of intravenous diuretics [34], and such maneuvers have been advocated, particularly in patients with GI, GU malignancies and abdominal lymphoma. The use of diuretics typically mandates bladder catheterization when scan table times approach an hour, as the patient typically will need to void during the scan without urinary bladder drainage. With scan table times well under 30 minutes, this is less problematic. When bladder catheterization is used, best results are obtained using a multi-lumen catheter such that the urinary bladder undergoes continuous lavage [35]. This insures a relatively full bladder with only dilute urinary tracer. Some centers report with aggressive hydration and use of diuretics, very little urinary tracer is present in the bladder at the time of imaging. In any case, the use of an indwelling urinary bladder catheter adds an invasive component to the exam, and requires skilled personnel time, and this must be weighted against the advantages of reducing or eliminating bladder urinary tracer activity.

Bowel FDG physiological tracer activity is commonly observed on whole-body FDG PET scans and can be confounding due to the inconsistent and unpredictable patterns [31, 35]. While the aetiology of this uptake is not entirely understood, maneuvers have been advocated to reduce or eliminate bowel tracer activity, including isosmotic bowel preparations the evening prior to the exam [34], or bowel smooth muscle relaxants prior to FDG administration [36]. These maneuvers must again be viewed in the context of patient compliance and increasing the complexity of the examination. Isosmotic bowel cleansing is demanding on the patient to say the least, and further, bowel FDG activity is usually readily identified on high quality PET images. In certain patients, however, such as ovarian carcinoma, abdominal lymphoma and colon cancer, where mesenteric or bowel serosal implants are possible, such preparation to eliminate or minimize bowel physiological tracer activity may well be indicated.

Muscle FDG uptake is also common physiological variant which can be confounding, particularly in the neck [31, 35]. As noted above, generalized muscle uptake due to insulin action can be eliminated by sufficient fasting and avoidance of exogenous insulin prior to FDG administration. Skeletal muscle contraction during the uptake phase of FDG (principally 30 minutes following intravenous administration) can result in fairly intense FDG accumulation, hence patients should be seated or recumbent following FDG administration, and not engaged in any physical activity for 20–30 minutes. Talking, chewing or swallowing should be avoided during this period, as this can result in FDG uptake in the tongue, muscles of mastication, and larynx [37]. Intense muscle activity prior to administration of FDG, even hours prior, can result in elevated muscle uptake as well, and hence patients are generally advised to avoid strenuous physical activity prior to undergoing an FDG PET scan. FDG uptake in major muscles of the neck including the sterno-cleido-mastoid and scalene muscles can be seen also be seen, and particularly with patients undergoing studies for malignancies involving the neck, a recumbent position with head support during the FDG uptake phase is commonly advocated. More confounding in the neck and supraclavicular region is brown adipose tissue (BAT) FDG uptake, originally thought to reflect physiological muscle uptake. Brown adipose fat is involved in thermoregulation, and on adrenergic stimulation, can accumulate FDG avidly [38]. Recognition of this source of confounding physiological uptake occurred with the advent of combined PET/CT scanners [39, 40]. Most typically seen in the lower neck, medial shoulders and paraspinal fat between muscle groups, brown adipose tissue uptake can be seen in mediastinal fat and subdiaphragmatic and perirenal fat [41]. Typically seen in younger and slimmer patients, particularly when cold, brown adipose tissue FDG uptake is often quite focal, and can be very difficult to distinguish from lymph node metastases without accurately registered and aligned images such as provided by combined PET/CT scanners. Anxiolytics have been shown to be effective in eliminating neck muscle and brown adipose fat uptake [42], presumably due to reduced muscle tension and diminished adrenergic stimulative output, respectively. Some centers keep patients warm with blankets or elevated ambient temperature as a strategy to reduce brown adipose fat uptake.

Anxiolytics, including intravenous short acting benzodiazepines such as midazolam, routinely in adult patients to improve patient comfort and compliance are used at some centers. With the substantially shorter whole-body imaging times of contemporary tomographs, however, the importance of such light conscious sedation has diminished. Certainly for patients with back pain or other impediments to maintaining motionless supine position during the scan acquisition, sedation and pain management entirely analogous to that used for MRI imaging is indicated. In general, there is far less difficulty with patient claustrophobia in whole-body PET acquisitions relative to closed magnet MRI acquisitions. Oral alprazolam, 05–1.5 mg, depending on body weight, an hour before scan acquisition, is very effective in managing patients with claustrophobia.

Image Acquisition

As with any clinical medical imaging procedure, the goal is to obtain the highest quality image in a limited image acquisition time in order to minimize patient movement and maximize scanner throughput. As noted above, in the past whole-body FDG PET images had been obtained without attenuation correction, less the total scan acquisition time exceed two hours. Contemporary PET scanners, and particularly combined PET/CT tomographs, allow whole-body attenuation corrected images routinely in as little as 30 minutes. As patient movement between the transmission and emission image acquisitions will result in artefacts on the final attenuation corrected emission images, the emission and transmission image acquisitions should be temporally as close as possible when sealed source transmission scans are used (Fig. 13.1). The patient's arms are a common source of movement artefact. Most patients can comfortably keep their arms up out of the torso field of view when properly supported for 30 minutes or less. For whole-body scan acquisitions on fast crystal (LSO or GSO) tomographs and combined PET/CT tomographs, where such short whole-body acquisition times are feasible, an arms up supine configuration is optimal for chest, abdomen and pelvis examinations. Head and neck image acquisitions are, as with CT, optimally performed with arms down.

Image acquisition times and FDG dose are related, but not in an entirely inverse fashion of single photon radiotracer medical imaging. Regarding sealed source transmission scans, with image segmentation, acquisition time per bed position can be shorted to 3 or even 2 minutes in conventional BGO whole ring tomographs, while sealed point sources using with fully 3D tomographs and higher activity rod sources used in fast crystal 2D tomographs allow for reduction in acquisition time to 2 minutes or less per bed position. Such short transmission acquisition times can result in segmentation errors, particularly associated with the diaphragm. CT based attenuation correction allows for the entire body transmission scan without noise or segmentation errors [43] in less than 30 seconds with multi-detector helical CT. Since the PET emission acquisitions are acquired after the single CT scan of the entire torso, the transmission image acquisition of the last portion of the body to undergo emission image acquisition may be separated by up to 30 minutes, hence absence of patient movement is essential. Also, shallow relaxed breathing will help minimize image registration errors when X-ray CT is used for the transmission image sinogram because even when the CT acquisition is performed during free breathing, the temporal relation about the diaphragm over seconds captured by CT will be different than the PET emission acquisition captured over a few to several minutes. This appears to be less of an issue with increasing number of detector channels with helical CT such as up to 16, as the increasing speed of CT scan acquisition reduces diaphragm motion artefact [44]. Alternatively, abdominal binders can be employed to constrain diaphragmatic excursion to minimize such errors. Mid exhalatory breath hold provides improved quality CT images and can closely match average diaphragmatic position on the PET images [45]. Patients short of breath due to pulmonary disease may benefit from supplemental oxygen to reduce lung tidal volume, and use of abdominal binders can aid in insuring shallow breathing.

Due to the nature of contaminating scatter and random coincidence events detected, the relationship between FDG dose and useable image counting statistics is neither direct nor linear, and depends on the geometry of the tomograph, type of detector crystal, size of the patient, and the reconstruction algorithm used. The general rule of single photon medical radiotracer imaging, that a larger radiopharmaceutical dose results in more useable counts, does not uniformly apply in whole-body PET imaging. Because random coincidences increase exponentially (to the second power) with tracer activity while true coincidences increase linearly with the tracer activity, useable count rates are eventually limited by randoms coincidence contribution. In general, ring tomographs in 2D mode with thick axial septa will increase useable true coincidences with increasing patient tracer activity (administered dose) out to the upper range of dosimetry limited [46] administered FDG (about 700 MBq).

Hence increasing administered dose can be used to reduce emission image acquisition times, from, for example, 8 minutes to 4 minutes per bed position. Tomographs with greater axial cross-plain acceptance and finer septa, and especially tomographs operating in fully 3D mode (no septa), may reach randoms limiting count rate contributions with administered doses as low as 300 MBq or less. Hence, increasing the dose of administered FDG above such levels does not allow for decreased scan acquisition times, indeed image degradation can be observed with increasing dose using the same scan acquisition times, as predicted by NEC curves [Fig. 13.4]. Likewise, larger patients provide an expanded source of photon emissions to the detector ring, resulting in higher randoms, especially in tomographs operating in 3D mode. Hence in a large patient a lower FDG dose with an extended image acquisition time can improve final image quality in tomographs operated in fully 3D mode. The 3D mode does result in substantial gains in sensitivity, however, such that useable true coincidence count rates are acquired with lower administered FDG in the range of 200–300 MBq. The fast crystal tomographs (LSO and GSO) allow for considerably narrower coincidence acceptance windows (4–6 nsec vs 8–12 nsec) than BGO or NaI(Tl) based tomographs, reducing relative random contributions by roughly half. The rapid light decay of such fast crystals also permits very high detector count rates, permitting 3D mode acquisitions using patient FDG doses well above 500 MBq (Fig. 13.4). Such tomographs in 3D mode yield useable increases in true coincidence count rates with administered doses of FDG in excess of 500 MBq, allowing emission image acquisitions to be shortened to 2–3 minutes per bed position (Fig. 13.5).

Photon scatter contributes to background noise in the reconstructed images and degrades image contrast in PET, just as with single photon radionuclide imaging. Larger patients will thus present greater image degradation due to a larger scatter component emanating from the patient. Again, 2D tomographs with thick septa will be less degraded by the increased scatter contribution than tomographs with more limited, or no, axial collimation, as with a fully 3D operation. Advances in scatter correction algorithms have greatly improved image quality, particularly in 3D mode (Figs. 13.2 and 13.3), by correcting for scatter coincidence contributions. In addition, refinements in energy resolution (raising the lower threshold of energy window from 350 keV to as high as 425 keV) has resulted in further improvements in reduce scatter contribution with attendant improvements in whole-body image quality in a 3D emission acquisition mode, even in large patients (Fig. 13.6).

A clear consensus of the optimal time for whole-body image acquisition following FDG administration has not yet emerged. Typically image acquisition for body imaging has commenced 40–60 minutes following FDG administration. This delay is based in part on the time required for a majority of blood pool activity to clear and the majority of the tumor accumulation of tracer to occur, and in part on the historical need to minimize the time between pre-injection transmission scans and the commencement of emission image acquisition. With whole-body imaging times up to and exceeding an hour, emission acquisition of the last portion of the body imaged can occur over two hours post tracer administration. There is continued accumulation of FDG in malignant neoplasms and other FDG avid tissues such as bone marrow beyond one hour, with continued clearance of blood pool [47]. Hence, a longer delay in the commencement of image acquisition has been advocated to enhance tumor conspicuity and allow for more complete clearance of upper urinary tract tracer activity. Upper urinary tract tracer activity in the absence of aggressive hydration and use of diuretics is not assured even at 2 hour post FDG administration [48], and an increase in tumor to background is offset by the physical decay of tracer, lowering counting statistics. For tomographs that are count rate limited or encounter dominating random coincidence contributions with FDG doses exceeding 300 MBq, a longer delay, such as 90–120 minutes, with a corresponding higher administered FDG dose may provide optimal whole-body imaging. For tomographs operated in 2D with relatively heavy septa or in 3D with fast scintillation crystals, the optimal dose of FDG and delay time has not yet been fully explored, but likely is between one and two hours. Increasingly centers are moving to 90 minute uptake times for routine body oncology imaging, and in some instances advocating uptake times of 2 to 3 hours for cancers with modest average FDG accumulation such as breast or pancreatic cancer.

Image Display and Interpretation

Whole-body FDG PET images routinely are displayed as a combination of a series of orthogonal tomographic images in the transaxial, coronal, and sagittal planes, and a whole-body rotating projection image. The rotating projection image provides an invaluable rapid assessment of the overall status of FDG avid malignancy in the body, and can be very helpful in discerning the three dimensional relationships of abnormalities to normal structures. Interpretation of

whole-body images is thus best accomplished using both the rotating whole-body projection image and the serial tomographic images. As noted above, emission only (non-attenuation corrected) images are being largely supplanted by attenuation corrected images, however as image reconstruction artefacts can occur due to patient movement between the emission and transmission image acquisitions, the non-attenuation corrected images can serve as a useful fall back set of images. Additionally, iterative image reconstruction methods can constrain some aspects of movement artefacts and noise into discrete focal abnormalities potentially mistaken for clinically significant abnormalities such as metastatic deposits. Consequently viewing non-attenuation corrected images reconstructed with conventional filtered back projection has been advocated as a routine adjunct or at least fall back set of images to the attenuation corrected images reconstructed with statistical reconstruction algorithms. There remains controversy over the use of semi-quantitative measures of FDG uptake in the setting of routine diagnostic FDG PET applications in oncology, with some centers using semi-quantitative measures such as the Standardized Uptake Value (SUV) routinely, while others rely entirely on visual interpretation. SUVs should be used with caution as an absolute criteria for malignancy, not only because the degree of FDG uptake implies a probability of malignancy, not an absolute threshold, but more importantly because SUVs reported in the literature are generally insufficiently standardized amongst different PET imaging laboratories to be universally applied [48]. When a patient undergoes serial PET imaging on the same tomograph a the same institution using the same imaging protocol to assess change in FDG uptake such as in the setting of therapy monitoring, SUV or similar semi-quantitative measurements may well be a very useful adjunct to visual interpretation, although current data regarding therapy monitoring with FDG PET suggests it is the complete resolution of abnormal FDG uptake (essentially a qualitative interpretation) that is most predictive of progression free survival [49].

Interpretation of PET and CT images generated by combine PET/CT scanners or by registered and aligned images of PET and CT images acquired on separate tomographs requires workstations capable of displaying both PET and CT images in full resolution (512×512 matrix for CT) and rapid stacked image display at full image fidelity for rapid and full interpretation of the PET and CT images, along with the rotating whole-body projection images. It should be noted that CT images produced by combined PET/CT scanners are fully diagnostic CT images, and hence interpretation of PET/CT involves both anatomical diagnosis based on CT images and metabolic diagnosis based on the PET images. The CT images, while used for anatomical reference and localization of abnormalities on the PET images to aid in PET interpretation, contain essential independent anatomical diagnostic information as well, and hence display of CT images must be displayed in full fidelity with rapid access to window and level settings as well as image reconstruction algorithms (soft tissue vs lung/bone). So-called fusion images, in which the CT and PET images are superimposed using gray scale for the CT and a color scale for the PET are of limited utility as the PET color image obscures the CT image and subtle findings on PET are obscured by the CT images. Side by side registered and aligned images in gray scale with coordinated cursors provides rapid access to all information on both images and permits efficient complete interpretation of both PET and CT image sets.

Conclusions

In as little as a decade whole-body PET imaging has emerged as an essential component of medical imaging in oncology. Rather than being a competitor of CT based anatomical diagnosis in body oncology imaging, the complimentary value of metabolic diagnosis provided by PET and anatomical diagnosis provided by CT is now manifest in combined PET/CT scanners, which likely will quickly become the standard for body oncology medical diagnosis.

References

1. Shreve PD. Status of clinical PET in the USA and the role and activities of the institute for clinical PET. In: Positron Emission Tomography: A Critical Assessment of Recent Trends. [Bulyas B and Muller-Gartner HW, Eds] Dordrecht: Kluwer 1998:33–42.
2. Phelps ME, Hoffman EJ, Mullani NA, Ter-Pogossian MM. Application of annihilation coincidence detection to transaxail reconstruction tomography. J Nucl Med 1975;16:210–224.
3. Ter-Pogossian MM, Phelps ME, Hoffman EJ, et. al. A positron-emission transaxial tomograph for nuclear medicine imaging (PETT). Radiology 1975;114:89–98.
4. Willimas, Crabtree, Burgiss. Design and performance characteristics of a positron emission computed axial tomograph-ECAT-II. IEEE Trans Nucl Sci 1979;26.
5. Hoffman EJ, Phelps ME, Huang S-C. Perfomance evaluation of a positron tomograph designed for brain imaging. J Nucl Med 1983;24:245–257.
6. Casey ME, Nutt R. A multicrystal two-dimensional BGO detector system for postiron emission tomography. IEEE Trans. Nucl Sci 1986;NS33:460–463.

7. Gupta NC, Frank AR, Dewan NA, et. al. Solitary pulmonary nodules: detection of malignancy with PET with 2-[F-18]-fluoro-2Deoxy-D-glucose. Radiology 1992;184:441–444.
8. Glaspy JA, Hawkins R, Hoh CK, Phelps ME. Use of positron emission tomography in oncology. Oncology 1993;7:41–50.
9. Price P. Is there a future for PET in oncology. Eur J Nucl Med 1997;24:587–589.
10. Wahl RL, Zasadny K, Helvie M, Hutchins GD, Weber B, Cody R. Metabolic monitoring of breast cancer chemohormonotherapy using positron emission tomography: initial evaluation. J Clin Onc 1993;11:2101–2111.
11. Rigo P, Paulus P, Kaschten BJ, et. al. Oncologic applications of positron emission tomography with fluorine-18 fluorodeoxyglucose. Eur J Nucl Med 1996;23:1641–1674.
12. Muehllehner G, Karp JS, Mankoff DA, Beerbohm, Ordonez CE. Design and performance of a new positron emission tomograph. IEEE Trans Nucl Sci 1988;35:670–674.
13. Karp JS, Muehllehner G, Qu H, Yan X-H. Singles transmission in volume-imaging PET with a ^{137}Cs source. Phys Med Biol 1995;40:929–944.
14. Townsend DL, Wensveen M, Byars LG, et. al. A rotating PET scanner using BGO block detectors: design, performance, and applications. J Nucl Med 1993;34:1367–1376.
15. Mullani NA, Gould KL, Hitchens RE, et. al. Design and performance of POSICAM 6.5 BGO positron camera. J Nucl Med 1990;31:610–616.
16. Wienhard K, Eriksson L, Grootoonk S, Casey M, Pietrzyk U, Heiss W. Performance evaluation of the positron scanner ECAT EXACT. JCAT 1992;16:804–813.
17. DeGrado TR, Turkington TG, Williams JJ, Stearns CW, Hoffman J, Coleman RE. Performance characteristics of a whole-body PET scanner. J Nucl Med 1994;35:1398–1406.
18. Hudson HM, Larkin RS. Accelerated image reconstruction using ordered subsets of projection data. IEEE Tans Med Imaging. 1994;13:601–609.
19. Xu M, Cutler PD, Luk WK. Adaptive, segmented attenuation correction for whole-body PET imaging. IEEE Trans Nucl Sci. 1996;43:331–336.
20. Wahl RW. To AC or not to AC: that is the question. J Nucl Med 1999;40:2025–2028.
21. Kinahan PE, Rogers JG. Analytic 3D image reconstruction using all detected events. IEEE Tans. Nucl. Sci. 1989;36:964–968.
22. Townsend DW, Geissbuhler A, Defrise M, et. al. Fully three-dimensional reconstruction for a PET camera with retractable septa. IEEE Tans. Med. Imaging 1991;MI-10:505–512.
23. Muehllehner G. Design considerations for PET scanners. Quarterly Journal of Nuclear Medicine. 2002;45: 16–23.
24. Watson CC. New, faster, image-based scatter correction for 3D PET. IEEE 2000;47:1587–1594.
25. Beyer T, Townsend DW, Brun T, et. al. A combined PET/CT scanner for clinical oncology. J Nucl Med 2000;41:1369–1379.
26. Shreve PD. Adding structure to function. J Nucl Med 2000;41:1380–1382.
27. Kinahan PE. Townsend DW, Beyer T, Sashin D. Attenuation correction for a combined 3D PET/CT scanner. Med. Phys. 1998;25:2046–2053.
28. Halpern B, Dahlbom M, Vranjesevic D, et. al. LSO-PET/CT whole-body imaging in 7 minutes: is it feasible? J Nucl Med 2003;44:380–381.
29. Bar-Shalom R, Yefremov N, Guralnik L, et. al. Clinical performance of PET/CT in evaluation of cancer: Additional value for diagnostic imaging and patient management. J Nucl Med 2003;44:1200–1209.
30. Cohade C, Osman M, Leal J, Wahl RL. Direct comparison of 18F-FDG and PET/CT in patients with colorectal carcinoma. J Nucl Med 2003;44:1797–1803.
31. Ollenberger GP, Weder W, von Schulthess GK, Steinert HC. Staging of lung cancer with integrated PET-CT. N Engl J Med 2004;350: 86–87.
32. Shreve, PD, Anzai Y, Wahl RW. Pitfalls in oncologic diagnosis with FDG PET imaging: Physiologic and benign variants. Radiographics 1999;19:61–67.
33. Lindholm P, Minn H, Leskinen-Kallio S, Bergman J, Ruotsalainen U, Joensuu H. Influence of the blood glucose concentration of FDG uptake in cancer: a PET study. J Nucl Med 1993;34:1–6.
34. Vesselle HJ, Miraldi FD. FDG PET of the retroperitoneum: normal anatomy, variants, pathological conditions, and strategies to avoid diagnostic pitfalls. RadioGraphics 1998;18:805–823.
35. Brigid GA, Flanagan FL, Dehdashti F. Whole-body positron emission tomography: normal variations, pitfalls, and technical considerations. AJR 1997;169:1675–1680.
36. Miraldi F, Vesselle H, Faulhaber PF, Adler LP, Leisure GP. Elimination of artifactual accumulation of FDG in PET imaging of colorectal cancer. Clin Nucl Med 1998;23:3–7.
37. Stahl A, Weber W, Avril N, Schwaiger M. The effect of N-butylscopolamine on intestinal uptake of F-18 fluorodeoxyglucose in PET imaging of the abdomen. Eur J Nucl Med 1999;26(P):1017.
38. Kostakoglu L, Wong JCH, barrington SF, Cronin BF, Dynes AM, Maisey MN. Speech-related visualization of laryngeal muscles with fluorine-18 FDG. J Nucl Med 1996;37:1771–1773.
39. Hany TF, Gharelpapagh E, Kamel E, Buch A, Himms-Hagen J, von Schulthess G. Brown adipose tissue: a factor to consider in symetrical tracer uptake in the neck and upper chest region. Eur J Nucl Med Mol Imaging 2002;29:1393–1398.
40. Cohade C, Osman M, Pannu HK, Wahl RL. Uptake in supraclavicular area fat ("USA-Fat"): Description on 18F-FDG PET/CT. J Nucl Med 2003;44:170–176.
41. Yeung HWD, Grewal RK, Gonen M, Schoder H, Larson SM. Patterns of 18-F FDG uptake in adipose tissue and muscle: A potential source of false-positives for PET. J Nucl Med 2003; 44:1789–1796.
42. Barrington SF, Maisey MN. Skeletal muscle uptake of fluorine-18-FDG: effect on oral diazepam. J Nucl Med 1996;37:1127–1129.
43. Beyer T. Personnel communication.
44. Beyer T, Antoch G, Muller S, Egelhof T, Freudenberg LS, Debatin J, Bockisch A. Acquisition protocol considerations for combined PET/CT imaging. J Nucl Med 2004;45:25S–35S.
45. Jones SC, Alavi A, Christman D, Montanez I, Wolf AP, Reivich M. The radiation dosimetry of 2-[F-18]fluoro-2Deoxy-D-glucose in man. J Nucl Med 1982;23:613–617.
46. Hamberg LM, Hunter GJ, Alpert NM, Choi NC, Babich JW, Fischman AJ. The dose uptake ratio as an index of glucose metabolism: useful parameter or oversimplification? J Nucl Med 1994; 35:1308–1312.
47. Lowe V. Personnel communication.
48. Keyes JW Jr. SUV: standard uptake value or silly useless value? J Nucl Med 1995;36:1836–1839.
49. Kostakoglu L, Goldsmith SJ. 18F FDG PET evaluation of the response to therapy for lymphoma and for breast, lung and colorectal carcinoma. J Nucl Med 2003;44:224–239.